Chinese Herbal Medicines 15 (2023) 398–406

Contents lists available at ScienceDirect

Chinese Herbal Medicines

journal homepage: www.elsevier.com/locate/chmed

Original Article

Glucuronic acid metabolites of phenolic acids target AKT-PH domain to improve glucose metabolism

Jie Gao [a], Manqian Zhang [a], Xingwang Zu [a], Xue Gu [a], Erwei Hao [b], Xiaotao Hou [b], Gang Bai [a,b,*]

[a] State Key Laboratory of Medicinal Chemical Biology, College of Pharmacy and Tianjin Key Laboratory of Molecular Drug Research, Nankai University, Tianjin 300353, China
[b] Guangxi Key Laboratory of Efficacy Study on Chinese Materia Medica, Guangxi Collaborative Innovation Center for Research on Functional Ingredients of Agricultural Residues, Guangxi University of Chinese Medicine, Nanning 530200, China

ARTICLE INFO

Article history:
Received 14 July 2022
Revised 8 October 2022
Accepted 3 November 2022
Available online 12 April 2023

Keywords:
AKT
glucuronic acid
glucose metabolism
metabolite
phenolic acid
PH domain

ABSTRACT

Objective: Phenolic acids widely exist in the human diet and exert beneficial effects such as improving glucose metabolism. It is not clear whether phenolic acids or their metabolites play a major role *in vivo*. In this study, caffeic acid (CA) and ferulic acid (FA), the two most ingested phenolic acids, and their glucuronic acid metabolites, caffeic-4′-*O*-glucuronide (CA4G) and ferulic-4′-*O*-glucuronide (FA4G), were investigated.

Methods: Three insulin resistance models *in vitro* were established by using TNF-α, insulin and palmitic acid (PA) in HepG2 cells, respectively. We compared the effects of FA, FA4G, CA and CA4G on glucose metabolism in these models by measuring the glucose consumption levels. The potential targets and related pathways were predicted by network pharmacology. Fluorescence quenching measurement was used to analyze the binding between the compounds and the predicted target. To investigate the binding mode, molecular docking was performed. Then, we performed membrane recruitment assays of the AKT pleckstrin homology (PH) domain with the help of the PH-GFP plasmid. AKT enzymatic activity was determined to compare the effects between the metabolites with their parent compounds. Finally, the downstream signaling pathway of AKT was investigated by Western blot analysis.

Results: The results showed that CA4G and FA4G were more potent than their parent compounds in increasing glucose consumption. AKT was predicted to be the key target of CA4G and FA4G by network pharmacology analysis. The fluorescence quenching test confirmed the more potent binding to AKT of the two metabolites compared to their parent compounds. The molecular docking results indicated that the carbonyl group in the glucuronic acid structure of CA4G and FA4G might bind to the PH domain of AKT at the key Arg-25 site. CA4G and FA4G inhibited the translocation of the AKT PH domain to the membrane, while increasing the activity of AKT. Western blot analysis demonstrated that the metabolites could increase the phosphorylation of AKT and downstream glycogen synthase kinase 3β in the AKT signaling pathway to increase glucose consumption.

Conclusion: In conclusion, our results suggested that the metabolites of phenolic acids, which contain glucuronic acid, are the key active substances and that they activate AKT by targeting the PH domain, thus improving glucose metabolism.

1. Introduction

Natural products are not only ingredients to be consumed, but also sensory signals to initiate related reaction pathways *in vivo* (Belwal, Nabavi, Nabavi, & Habtemariam, 2017; Lee et al., 2022). Phenolic acids (hydroxycinnamic and hydroxybenzoic acids) widely exist in natural products, particularly those used for medical purposes, which are known as herbal medicines (Kumar & Goel, 2019). For example, phenolic compounds, especially caffeic acid (CA) and ferulic acid (FA), are the major antioxidant constituents in *Angelicae Sinensis Radix* (Danggui in Chinese) (Li, Wu, & Huang, 2009). In addition, human daily diets, such as grains, vegetables, fruits and other types of food and beverages including tea, coffee and wine, are all rich sources of polyphenols. An adult's average daily intake of phenolic acid is more than 600 mg, of which CA and FA are the most ingested, accounting for approximately 80% of the total phenolic acid intake (Ovaskainen et al., 2008). The beneficial effects of phenolic acids have been reviewed (Zhan et al., 2021). For example, the phenolic acid fraction from the extract of

* Corresponding author.
E-mail address: gangbai@nankai.edu.cn (G. Bai).

https://doi.org/10.1016/j.chmed.2022.11.005
1674-6384/

Sonchus oleraceus Linn, mainly containing chlorogenic acid and CA, improves insulin sensitivity in HepG2 cells (L. Chen, Teng, & Cao, 2019). Whether phenolic acid compounds play a regulatory role in the body is a topic worth exploring.

CA and FA exert anti-oxidant, anticancer, anti-inflammatory, anti-Alzheimer's disease and anti-diabetic effects. For example, CA exerts anticancer properties, at least partly through its anti-oxidant and pro-oxidant activities (Espindola et al., 2019). CA was shown to protect against acrolein-induced neurotoxicity in mouse hippocampal cells by activating AKT (also known as protein kinase B, PKB)/glycogen synthase kinase 3β (GSK3β) pathway and modulating the mitogen-activated protein kinase (MAPK) pathway (Huang et al., 2013). In addition, Chang et al. found that CA could upregulate the brain expression of proteins related to leptin and insulin signaling, such as phosphatidylinositol 3-kinase (PI3K), AKT, and glucose transporter 3 (GLUT3), in high-fat diet rats, thereby reducing serum glucose, insulin and leptin levels (Chang, Kuo, Chen, Wu, & Shen, 2015). FA can increase the activity and mRNA expression of enzymes involved in oxidation resistance, thereby scavenging free radicals and displaying a powerful antioxidant feature (Xie et al., 2020). FA can also improve blood glucose and serum insulin levels in rats with type 2 diabetes induced by high fat and fructose, increase phosphoenolpyruvate carboxykinase and glucose-6-phosphatase activities, and maintain normal glucose homeostasis (Narasimhan, Chinnaiyan, & Karundevi, 2015). Recently, Yin et al. reported the possible binding between FA and AKT, indicating its participation in the mechanism underlying the neuroprotective effect of FA in PC12 cells (Yin et al., 2019).

After entering the body, CA and FA can be quickly absorbed in the stomach, jejunum, and ileum, and then metabolized into glucuronic acid, sulfate and sulfonic glucuronic acid in the liver by sulfotransferase and uridine diphosphate glucuronosyltransferase (Lafay, Morand, Manach, Besson, & Scalbert, 2006; Pereira-Caro et al., 2016). These metabolites and unaltered free CA and FA circulate in the circulatory system and reach throughout the body (Zhao & Moghadasian, 2008). The concentration and duration of the metabolites maintained in the body are crucial to the *in vivo* activities of the compounds. Studies have shown that CA glucuronides are the main plasma metabolites after oral administration of CA, accounting for approximately 41% of all plasma metabolites after 2 h of administration (Azuma et al., 2000). Omar et al. reported that among the metabolites, caffeic-4′-*O*-glucuronide (CA4G) constituted approximately 42% in the urine sample of 0–24 h, while caffeic-3′-*O*-glucuronide constituted < 5%. They found that the liver was one of the major tissues outside the gastrointestinal tract, only secondary to the kidneys (Omar et al., 2012). Notably, the structures of CA and FA are very similar. This suggested that FA might share parallel metabolic processes and metabolites with CA, with ferulic-4′-*O*-glucuronide (FA4G) being one of its major metabolites *in vivo*. Zhao et al. reported that conjugated FAs, including FA-glucuronide, are the major metabolites in the plasma and urine of rats (Zhao & Moghadasian, 2008). FA is metabolized mainly in the liver, and it might undergo enterohepatic circulation, prolonging the presence of FA and its metabolites in the body to some extent (Zhao, Egashira, & Sanada, 2004). However, there are scarcely any reports of the pharmacological effects of these metabolites.

Studies have shown that after a compound is metabolized, the metabolites might have stronger activity than their parent compound. For example, the glucuronidated metabolites of bisphenol A (BPA) and bisphenol S (BPS) were reported to change the energy metabolism of neutrophils and certain antimicrobial reactions, and affect endocrine activity even more potently than BPA and BPS (Peillex, Kerever, Lachhab, & Pelletier, 2021). The secondary metabolites of quercetin can inhibit the activity of xanthine oxidoreductase, thereby reducing the plasma uric acid content in patients with hyperuricemia (Tumova, Shi, Carr, & Williamson, 2021). Grape seed extract rich in flavonoids exerts an anti-Alzheimer's disease effect that is not directly related to the flavonoids in the diet, but related to their secondary metabolites, especially glucuronidated metabolites (Docampo-Palacios et al., 2020).

Considering the possibility that metabolism might increase the efficacy of compounds, the metabolites CA4G and FA4G are supposed to be more potent in regulating glucose metabolism than their parent compounds. However, this hypothesis has not been testified. In this study, we compared the biological effects of the metabolites with their parent compounds, focusing on glucose consumption. Then, the targets of the metabolites were predicted by network pharmacology and verified by confirmation experiments. The comparison of the regulatory effects between these metabolites and their parent compounds in glucose metabolism, as well as the clarification of the underlying mechanism, will provide more evidence for the application of functional foods in the amelioration of glucose metabolism disorders. This will also lead to the research and development of novel compounds in the future.

2. Materials and methods

2.1. Materials and reagents

CA (C108308) and FA (F103702) (purity > 98.5%, determined by HPLC) were purchased from Aladdin (Beijing, China). CA4G (C080020) and FA4G (F308910) were purchased from Toronto Research Chemicals (Toronto, Canada). Palmitic acid sodium salt (PA, P-0208429) was purchased from Heowns (Tianjin, China). Human TNF-α (AF-300-01A-100) was purchased from PeproTech Inc. (NJ, USA). Insulin from bovine pancreas (I8040) and 1,1′-diocta decyl-3,3,3′,3′-tetramethylindocarbocyanine perchlorate (Dil, D8700) were purchased from Solarbio (Beijing, China). Metformin hydrochloride (Met, B25331) was sourced from Shanghai Yuanye Bio-Technology Co., Ltd. (Shanghai, China). The primary antibodies for AKT (cat no. 4691S), GSK3β (cat no. 12456S) and the anti-rabbit IgG (cat no. 7070S), were purchased from Cell Signaling Technology (Massachusetts, USA). Antibodies against p-AKT (phospho-T308, ab38449), p-AKT (phospho-S473, ab8932) and glyceraldehyde-3-phosphate dehydrogenase (GAPDH, ab181602) were purchased from Abcam (Cambridge, UK). A GSK3β (phospho-Ser9) polyclonal antibody (BS94042) was purchased from Bioworld Technology (Minnesota, USA). SC79 was purchased from MedChemExpress (MCE, NJ 08852, USA). Two plasmids with the pleckstrin homology (PH) domain, i.e., pcDNA3-AKT-PH-GFP (PH-GFP, #18836) and pcDNA3-AKT-PH [R25C]-GFP (R25C, #18837), were purchased from Addgene (MA, USA). All cell culture reagents were obtained from Gibco BRL Life Technologies (Grand Island, NY, USA). All the other chemicals used were of analytical grade.

2.2. Cell culture

HepG2 and HEK 293T cells were acquired from American Type Culture Collection (Rockville, MD), and cultured in Dulbecco's modified Eagle's medium (DMEM) with 100 U/mL penicillin, 100 μg/mL streptomycin and 10% (volume percent) fetal bovine serum. The cells were cultured in a 37 °C constant temperature incubator with 5% CO_2.

2.3. In vitro insulin resistance models

Hyperinsulinemia can induce insulin resistance. Similarly, high levels of free fatty acids (FFAs) may also cause the secretion of inflammation-related cytokines and impair insulin sensitivity. In

addition, TNF-α is used in multiple signal transduction nodes by direct and indirect mechanisms through insulin action, thus playing an important role in obesity-induced insulin resistance. Therefore, three *in vitro* insulin resistance models were established according to our previous work (Zhang et al., 2019). Briefly, HepG2 cells in the logarithmic growth phase were cultured in 96-well culture plates. After the cells grew adherently, the medium in 96-well culture plates was discarded, and the cells were washed with precooled phosphate buffered solution (PBS) three times. Then, the three kinds of insulin resistance models were established by treating HepG2 cells with 1 μmol/L insulin for 36 h, 300 μmol/L PA for 24 h, or 20 ng/mL TNF-α for 24 h, respectively.

2.4. Glucose consumption assay

After treatment with insulin, PA or TNF-α for 24 h, HepG2 cells were incubated with CA (10, 1, and 0.1 μmol/L), CA4G (10, 1, and 0.1 μmol/L), FA (10, 1, and 0.1 μmol/L), FA4G (10, 1, and 0.1 μmol/L), or Met (10 μmol/L) as a positive control for another 12 h. Then, the supernatants were collected and measured according to the manufacturer's instructions with a Glucose Assay Kit (Zhongsheng Beikong Biotechnology Limited Company, Beijing, China). Glucose consumption levels were calculated by subtracting the glucose concentration of each group of supernatants from the glucose concentration of the medium (cell-free) and then normalized to the cell number using the MTT assay (Zhang, Yan et al., 2019).

2.5. Target prediction and molecular docking

The three-dimensional structures of CA4G and FA4G were input into the PharmMapper database (https://www.lilab-ecust.cn/pharmmapper/submitfile.html). The predicted human genes with fit values greater than 2.6 were selected and overlapped with the top 100 genes related to glucose metabolism obtained from the GeneCards database (https://www.genecards.org/). Then, the first 10 related pathways and 16 interacting proteins were analyzed through Kyoto Encyclopedia of Genes and Genomes (KEGG) (https://bioinfo.capitalbio.com) and String 9.1 (https://www.string-db.org/). The protein–protein interaction network analysis was visualized using Cytoscape (version 3.7.1) (Chen et al., 2020).

The three-dimensional crystal structure of the predicted protein target was obtained from the Protein Data Bank (PDB, https://www.rcsb.org/pdb). The creation of the structures of the molecules and the minimization of the energy were performed by SYBYL software (Chemical Computing Group, Inc.). The molecular docking of CA, CA4G, FA and FA4G with the AKT PH domain (PDB: 1UNQ) was performed with AutoDock software version 4.2 (Olson Laboratory, La Jolla, CA) as previously described (Gao et al., 2018). The distance between molecules was calculated by PyMOL 2.3.

2.6. Fluorescence quenching measurement

Specifically, the solutions of AKT protein, expressed in our laboratory (Zhang et al., 2020), at 5 μmol/L (in PBS buffer, pH 7.6) and of the small molecules CA, CA4G, FA, or FA4G at concentrations from 5 to 100 μmol/L were added in equal amounts to each well in 96-well plates and mixed adequately. Then, the mixtures were excited at 260 nm, and the fluorescence intensity at 308 to 400 nm at 37 °C was determined using a Cary Eclipse spectrofluorometer (Varian, Palo Alto, CA, USA). The interactions between the compounds and AKT proteins were expressed as dissociation constants (K_D) (Wang et al., 2019). The formula used for the calculation is as follows (Lakowicz & Weber, 1973).

$$\frac{1}{F_0 - F} = \frac{1}{F} + \frac{K_D}{F_0[Q]}$$

where F_0 and F are the fluorescence intensity of AKT solution at 328 nm in the absence and presence of drugs, respectively, and [Q] is the final concentration of drugs in the system. All tests were repeated three times.

2.7. Membrane translocation of pH domain

HEK 293 T cells were seeded in glass-bottomed dishes (MatTek, MA, USA), and treated with 10 μmol/L SC79 for 0.5 h or treated with CA (10, 1, and 0.1 μmol/L), CA4G (10, 1, and 0.1 μmol/L), FA (10, 1, and 0.1 μmol/L), or FA4G (10, 1, and 0.1 μmol/L) for 6 h. After washing once with PBS, cells were transfected with R25C or PH-GFP plasmid, which was used to indicate the cellular localization of the transfected fluorescent AKT PH domain protein with or without mutation, respectively, in a 37 °C incubator for 6 h. The cells were observed under a confocal microscope after incubation with 5 μmol/L Dil, a membrane dye, at 37 °C for 10 min. The excitation and emission wavelengths of GFP were 488 nm and 507 nm, respectively. The excitation and emission wavelengths of Dil were 549 nm and 565 nm, respectively.

The Pearson correlation coefficient was calculated by ImageJ software (Wayne Rasband, NIH, USA) with a Pearson correlation coefficient (PCC) colocalization plug.

2.8. Enzymatic activity determination

HepG2 cells were cultured in 75 cm^2 culture flasks at a density of 5×10^6 cells per flask and grown to 80% confluence. The cells were treated with CA4G (10, 1, and 0.1 μmol/L), FA4G (10, 1, and 0.1 μmol/L) or SC79 (10 μmol/L) for 6 h. Then, the protein concentration was quantified using a BCA protein assay kit (Solarbio, Beijing, China). According to the manufacturer's instructions, the absorbance at 340 nm was detected continuously to calculate the enzymatic activity of AKT in the cell lysates (GENMED, Arlington, MA, USA).

2.9. Western blotting

HepG2 cells were treated with FFA to establish the insulin resistance model. Then, the cells were treated with SC79 (10 μmol/L), CA (10, 1, and 0.1 μmol/L), CA4G (10, 1, and 0.1 μmol/L), FA (10, 1, and 0.1 μmol/L), or FA4G (10, 1, and 0.1 μmol/L) respectively for 2 h, according to our preliminary experiment (data not shown). Total proteins were extracted with a RIPA lysis buffer system (Solarbio, Beijing, China). Western blotting was performed routinely. The bands were visualized using Immobilon® Western Chemfluminescent HRP Substrate (Merck Millipore, USA) and analyzed by ImageJ software.

2.10. Statistical analysis

The data are expressed as the mean values ± standard deviations (SD). One-way analysis of variance (ANOVA) followed by Dunnett's post-hoc test was performed by the SPSS 11.5 program (SPSS Inc., Chicago, Illinois, USA) to compare the differences among groups. When the P value was < 0.05, the difference was considered statistically significant.

3. Results

3.1. CA4G and FA4G exert stronger effects on glucose consumption than CA and FA

To compare the effects of different treatments on glucose metabolism *in vitro*, glucose consumption by the cells was calculated. As shown in Fig. 1, glucose consumption was markedly reduced in the model group. Similar to Met, CA and CA4G improved glucose consumption in a dose-dependent manner (Fig. 1A–C). In insulin and FFA models, the effects of middle- and high-doses of CA4G were stronger than those of CA at the same doses. In the TNF-α model, the effect of high-dose CA4G was stronger than that of CA. These results showed that the activity of CA4G, the metabolite of CA, exerted more potent effects on improving glucose metabolism than CA. Similarly, FA4G was better than FA in increasing glucose consumption in these three insulin resistance models (Fig. 1D–F). Since CA4G and FA4G are both glucuronic acid metabolites of phenolic acid compounds and have similar structures, it was speculated that they might have a common mechanism of action.

3.2. CA4G and FA4G target AKT by binding to PH domain

The PharmMapper database was used to predict the potential target proteins of CA4G and FA4G. The genes from PharmMapper and disease-related genes in the GeneCards database were overlapped to further screen targets related to glucose metabolism (Fig. 2A). According to the false discovery rate, the first 10 pathways with the lowest value were selected, including the adenosine 5′-monophosphate-activated protein kinase signaling pathway, insulin signaling pathway, forkhead box O signaling pathway, insulin resistance, and PI3K-AKT signaling pathway (Fig. 2B). Then, Cytoscape software was used to analyze the relationship between selected pathways and targets. The size of the map node and edge were positively correlated with the degree and combined score. AKT, the largest node, was predicted to be the target of CA4G and FA4G (Fig. 2C).

Previous studies have indicated that the PH domain of AKT is an important active region, whose mutation or deletion can lead to a decrease or loss of AKT activity (Takeuchi et al., 1997). Therefore, we focused on the AKT PH domain to explore the interaction between the compounds and AKT. With the addition of small molecules, the endogenous fluorescence intensity of a protein decreases accordingly. This provides a clue for determining the interaction between them. Fluorescence spectroscopy was used to analyze the quenching effect of CA, CA4G, FA, and FA4G on the endogenous fluorescence of AKT. The maximal fluorescence emission peak of the AKT PH domain was at 328 nm. The K_D values of CA and CA4G at 328 nm were 182.8 μmol/L and 37.9 μmol/L, respectively. In addition, the K_D values of FA and FA4G at 328 nm were 185.1 μmol/L and 48.1 μmol/L, respectively. The K_D value indicated the combination strength between the compound and protein. These results signified that the binding between the metabolites and AKT was stronger than that between their parent compounds and AKT (Fig. 2D).

Then, we focused on the mode of binding between the compounds and the AKT PH domain to further investigate the mechanisms underlying the different interaction abilities. Molecular docking was performed by AutoDock 4.2 (Fig. 2E). In our results, there were hydrogen bonds between CA and several residues of the AKT PH domain, i.e., Asn-53, Glu-17, Tyr-18, Ile-19, Arg-23, and Lys-14. FA might interact with Asn-53, Glu-17, Tyr-18, Ile-19, Arg-23, and Lys-14 in the binding pocket. However, CA4G and FA4G might interact with AKT in a different way. They were

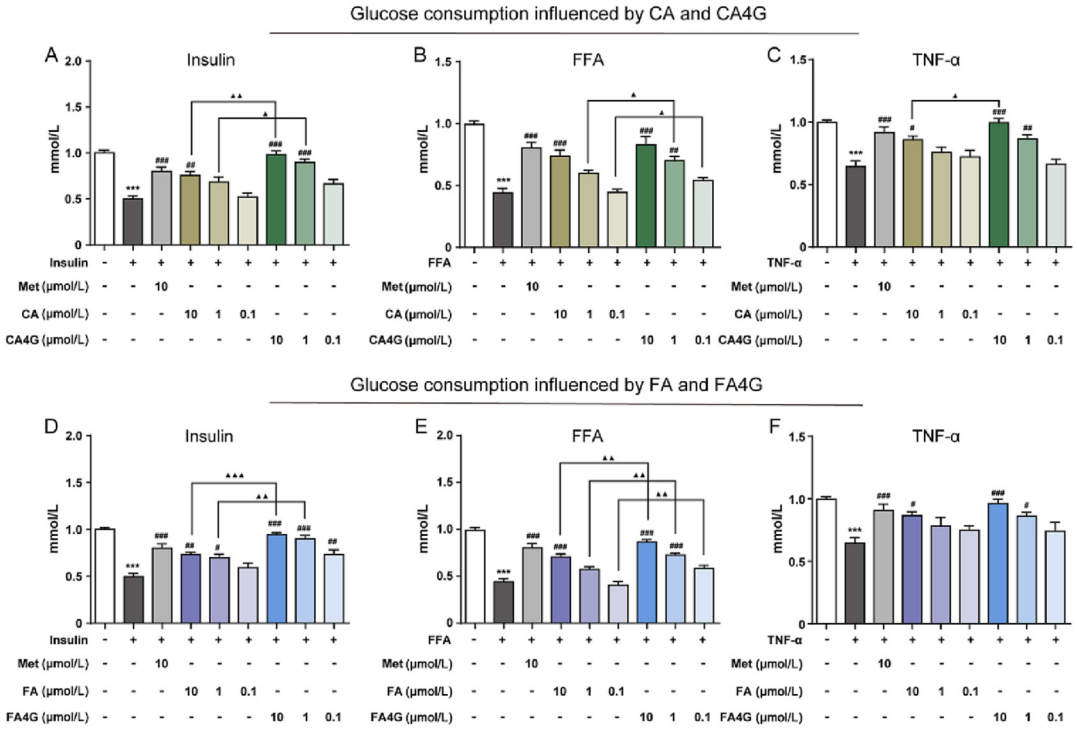

Fig. 1. Effects of CA, CA4G, FA and FA4G on glucose consumption in three insulin resistance models. Met was used as the positive control. (A) Effects of CA and CA4G on glucose consumption in insulin-stimulated HepG2 cells. (B) Effects of CA and CA4G on glucose consumption in FFA-stimulated HepG2 cells. (C) Effects of CA and CA4G on glucose consumption in TNF-α-stimulated HepG2 cells. (D) Effects of FA and FA4G on glucose consumption in insulin-stimulated HepG2 cells. (E) Effects of FA and FA4G on glucose consumption in FFA-stimulated HepG2 cells. (F) Effects of FA and FA4G on glucose consumption in TNF-α-stimulated HepG2 cells. The values are presented as the means ± SD (n = 6) ($^{***}P < 0.001$ *vs* control group; $^{\#}P < 0.05$, $^{\#\#}P < 0.01$, $^{\#\#\#}P < 0.001$ *vs* respective insulin resistance model group; $^{\blacktriangle}P < 0.05$, $^{\blacktriangle\blacktriangle}P < 0.01$, $^{\blacktriangle\blacktriangle\blacktriangle}P < 0.001$ *vs* respective parent compound group at the same dose).

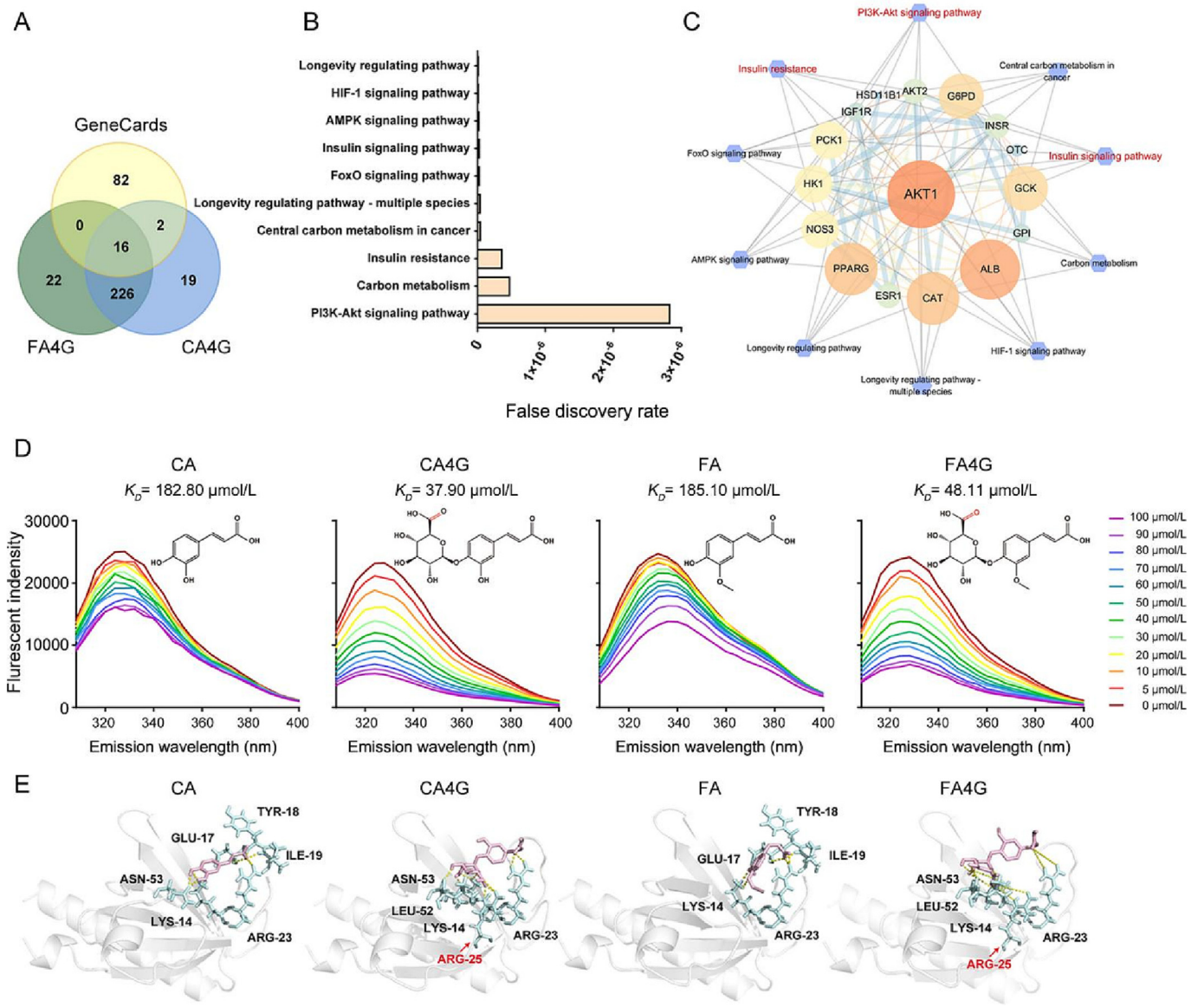

Fig. 2. Target of CA4G and FA4G is AKT. (A) Venn-diagram of the predicted targets of CA4G and FA4G by overlapping the genes from PharmMapper with glucose metabolism-related genes in the GeneCards database. (B) CA4G and FA4G related pathway scoring and functional analysis. (C) Protein–protein interaction network analysis of CA4G and FA4G targets with the first ten pathways. (D) The fluorescence quenching spectra of the AKT PH domain influenced by CA, CA4G, FA, and FA4G (ranging from 5 to 100 μmol/L). The concentration of the AKT PH domain was fixed at 5 μmol/L, and the ratios of CA, CA4G, FA, FA4G and the AKT PH domain were from 1:1 to 20:1. The vertical axis and the horizontal axis represent the fluorescence intensity and emission wavelength, respectively. The excitation wavelength was 260 nm, and the AKT emission peak was 328 nm. (E) Molecular docking of CA, CA4G, FA, and FA4G with the AKT PH domain. The distances between Arg-25 and O of the carbonyl group in CA4G were 2.0 and 2.1 Å, respectively, and were 2.5 and 2.6 Å between Arg-25 and O of the carbonyl group in FA4G.

both predicted to bind to the residues Asn-53, Arg-23, Lys-14, Arg-25, and Leu-52 in the AKT PH domain. Among these residues, Lys-14, Arg-25 and Arg-86 have been reported to be the three important sites related to AKT activity (Thomas, Deak, Alessi, & van Aalten, 2002). Moreover, in these three important residues, Arg-25 was the only different residue when comparing the predicted binding sites between the metabolites and their parent compounds. The results of molecular docking showed that the glucuronic acid structure of the metabolites could form hydrogen bonds with Arg-25. This might be the reason for the different effects between the parent compounds and their glucuronic acid metabolites. Considering the importance of Arg-25 on AKT activity, we focused on Arg-25, which was reported to be critical in membrane translocation (Thomas, Deak, Alessi, & van Aalten, 2002).

3.3. CA4G and FA4G activate AKT after binding to its PH domain

The activation of AKT can be roughly divided into two pathways. One pathway is to be recruited to the plasma membrane after binding to phosphatidylinositol (3,4,5)-trisphosphate (PIP_3) and phosphatidylinositol-4,5-bisphosphate (PIP_2), followed by phosphorylation at T308 and S473 (Badolia, Manne, Dangelmaier, Chernoff, & Kunapuli, 2015). The other pathway is to be directly activated in the cytoplasm without membrane translocation (Jo et al., 2012). The aforementioned results predicted that CA4G and FA4G would bind to the PH domain of AKT, which likely involved Arg-25. Therefore, the membrane translocation of AKT was examined. We performed membrane translocation assays of the AKT PH domain with the help of the PH-GFP plasmid. For the HEK 293T cells of the control group transfected with the PH-GFP plasmid,

obvious green fluorescence could be observed on the membrane, indicating the translocation of AKT to the plasma membrane. SC79, an AKT activator enhancing the phosphorylation of AKT, inhibited its transfer to the membrane after binding with the AKT PH domain. In addition, R25C is a PH domain mutant with an arginine to cysteine mutation at amino acid 25, resulting in the loss of the physiological function of membrane translocation of the AKT PH domain. R25C was used as a control to show the inhibition of AKT translocation. The results indicated that CA4G and FA4G bound to the AKT PH domain and inhibited its translocation to the cell membrane, similar to SC79 (Fig. 3A). The Pearson correlation coefficient was used to quantify the colocalization ratio of AKT PH domain fluorescence and membrane fluorescence. CA4G and FA4G had a dose-dependent inhibitory effect on the membrane translocation of the AKT PH domain, while CA and FA had no such effect, which further confirmed that CA4G and FA4G might have similar binding effects to the AKT PH domain (Fig. 3B).

Next, we used enzymatic activity determination to investigate the effects of CA4G and FA4G on AKT after binding to its PH domain. As shown in Fig. 3C, both CA and CA4G significantly increased AKT enzymatic activity in a dose-dependent manner. Compared to CA at the same dose, the metabolite CA4G exerted a relatively more potent effect in increasing AKT activity. Considering the above result of the membrane translocation of AKT, this result indicated that CA4G might activate AKT by inhibiting its translocation to the cell membrane, as SC79 did. Similarly, FA4G increased the enzymatic activity of AKT after inhibiting AKT translocation (Fig. 3D).

3.4. CA4G and FA4G regulate AKT signaling pathway

When AKT is activated, phosphorylation occurs at two sites, i.e., p-AKT (T308) and p-AKT (S473). Then, the AKT-GSK3β pathway is activated to participate in the process of glucose metabolism. To confirm the activation of AKT by CA4G and FA4G, we tested the phosphorylation levels of AKT and its downstream molecule, GSK3β. The results showed that CA4G and FA4G obviously increased the content of p-AKT (T308), p-AKT (S473) and p-GSK3β in a dose-dependent manner (Fig. 4). This confirmed the activation of AKT by CA4G and FA4G, and indicated that they might activate the downstream AKT-GSK3β pathway to exert their role in regulating glucose metabolism.

4. Discussion

In this study, CA4G and FA4G, the metabolites of CA and FA, were demonstrated to exert more potent effects on regulating glucose metabolism than their parent compounds. They might interact with Arg-25 in the AKT PH domain with a higher affinity than their parent compounds due to the glucuronic acid structure. After binding to AKT PH domain, CA4G and FA4G inhibited the membrane translocation of AKT, and activated it and its downstream signaling pathway, thus regulating glucose metabolism.

AKT, a serine/threonine kinase, is the main effector of the insulin signaling pathway and the PI3K signaling pathway. AKT is a key protein kinase required to maintain blood glucose concentration (Boucher, Kleinridders, & Kahn, 2014). It can change glucose and lipid metabolism in cells (Manning & Cantley, 2007) and regulate systemic glucose homeostasis, including glucose transport in fat and muscle cells (Jiang et al., 2003), and liver gluconeogenesis inhibition (Titchenell et al., 2016). As demonstrated in Fig. 5, growth factors such as insulin induce PI3K activation through receptor tyrosine kinase (RTK), including insulin receptor (INSR) and insulin-like growth factor 1 receptor (IGF1R), or G protein-coupled receptor (GPCR). Typical AKT activation is initiated by plasma membrane recruitment and activation of PI3K. PI3K can phosphorylate PIP_2 to produce PIP_3. Inactive AKT in the cytoplasm is recruited to the membrane to bind with PIP_3. The binding leads to the exposure of the T308 and S473 sites, which are phosphorylated by phosphoinositide dependent protein kinase 1 (PDK1) and mammalian target of rapamycin (mTOR) complex 2 (mTORC2) respectively, causing complete activation of AKT (Manning & Toker, 2017). After AKT is activated, it can phosphorylate and thus inhibit glycogen synthase kinase GSK3β, which inhibits the activation of glycogen synthase (GYS), to stimulate glycogen synthesis, thereby regulating glucose metabolism.

The structure of AKT mainly includes a C-terminal regulatory domain, an *N*-terminal PH domain, and a catalytic kinase domain in the middle. It facilitates the binding of AKT to PIP_3 on the membrane. In fact, in addition to the typical activation, AKT can also be activated in the cytoplasm. The AKT PH domain binds to agonists in the cytoplasm to expose the T308 and S473 sites, which are phosphorylated by PDK1 and mTORC2, respectively, resulting in complete activation of AKT (Jo et al., 2012). Studies have shown that after Arg-25, Lys-14 or Arg-86 of the AKT PH domain are mutated, the interaction between AKT and PIP_3 nearly disappears. Mutated AKT cannot be phosphorylated and activated by PDK1 even in the presence of PIP_3 (Thomas, Deak, Alessi, & van Aalten, 2002). Here, we found that the glucuronic acid structure of CA4G and FA4G could bind to the PH domain of AKT due to the interaction of the carbonyl group in glucuronic acid with Arg-25 in AKT. This induced the change in AKT structure in a direction that was favorable for phosphorylation, thereby bypassing the PIP_3-mediated AKT plasma membrane recruitment, and activating AKT in the cytoplasm.

Our results demonstrated that the compounds with glucuronic acid structures exerted biological activities by interacting with the AKT PH domain. This was in accordance with our previous reports showing that baicalin and chlorogenic acid, two compounds with glucuronic acid structures, can bind to Arg-25 of the AKT PH domain, inhibit the membrane translocation of AKT, activate AKT, and ultimately induce phosphorylation of downstream GSK3β to improve glucose metabolism (Gao et al., 2018; Yang et al., 2019). Furthermore, our previous research found that the glucuronic acid metabolites of two flavonoids, kaempferol and quercetin, also exerted more potent effects on improving glucose metabolism than their parent compounds due to binding to the AKT PH domain (Fang et al., 2021). This further confirmed the vital role of glucuronic acid in activating AKT. Notably, the structure of the PH domain exists not only in AKT but also in many other proteins, such as Bruton's tyrosine kinase (Btk) and Grb2-associated binder 1 (Ferguson et al., 2000). These proteins are crucial to many biological activities *in vivo*. Polyphenols have been reported to be beneficial due to the regulation of proteins containing the PH domain. For example, Tsai et al. reported the inhibition of Btk phosphorylation by resveratrol, which participated in the attenuation of lung injury (Tsai, Chen, Chang, Syu, & Hwang, 2019). Resveratrol was also reported to activate the Akt/GSK3β pathway, leading to protection of cardiomyocytes against anoxia/reoxygenation-induced injury (Tian et al., 2019). However, the mechanisms were not thoroughly investigated. It is reasonable to speculate that the metabolites might also act on the proteins containing the PH domain due to the glucuronic acid structure. Therefore, our future investigation focusing on the interaction between glucuronic acid metabolites and proteins containing the PH domain might broaden the application of polyphenols and their metabolites.

Notably, although PI3K/AKT/mTOR signaling is important in normal cellular processes, its aberrant activation participates in many human cancers. For example, lysosomal AKT inhibition has been used in the clinical treatment of metastatic cancer (Radisavljevic, 2020). However, AKT activation could also partici-

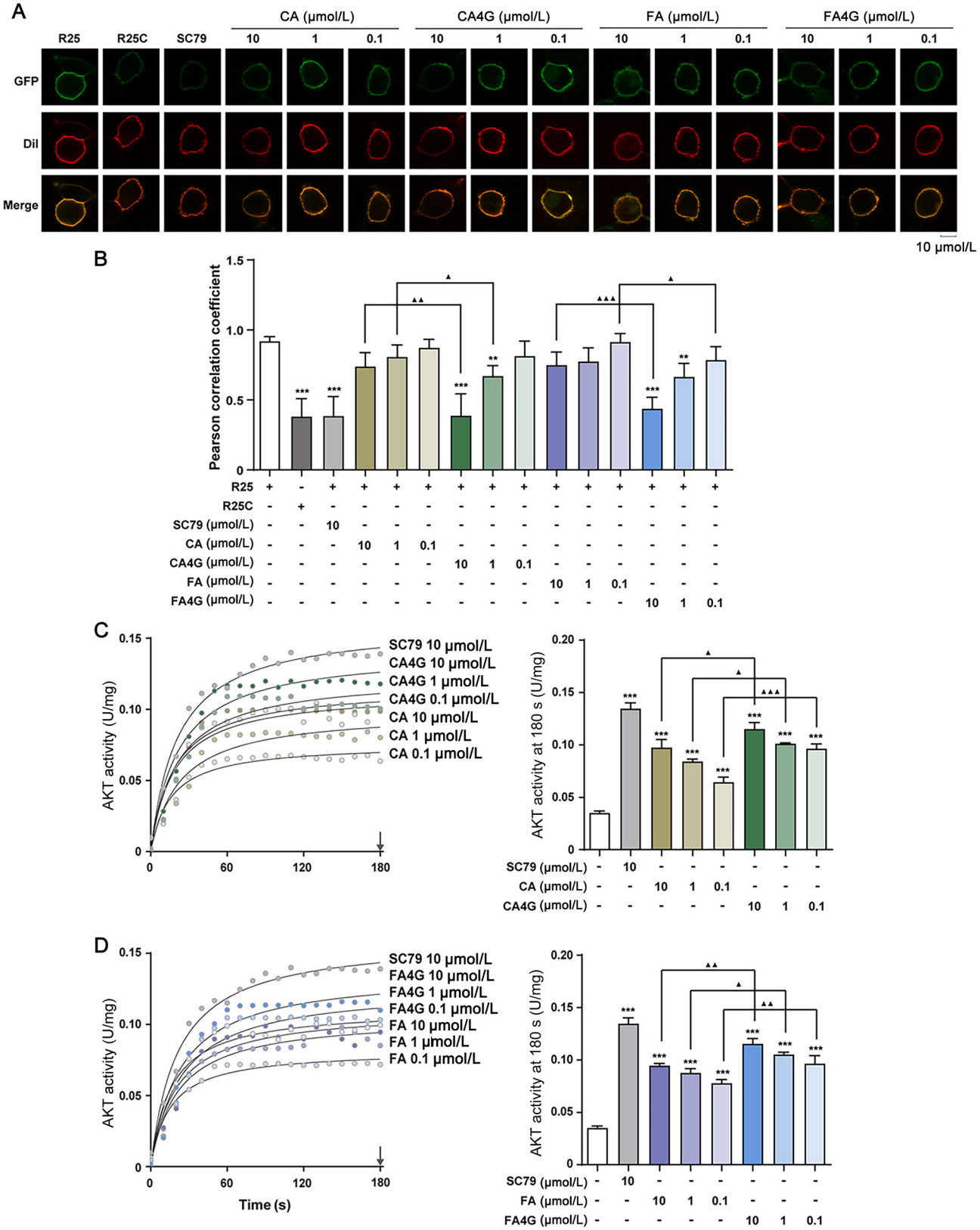

Fig. 3. CA4G and FA4G inhibited membrane translocation and increased the enzymatic activity of AKT. SC79 was used as the positive control to demonstrate AKT activation without membrane translocation. (A) Confocal images of CA, CA4G, FA, and FA4G influencing the membrane translocation of AKT. R25C was used as the control to show the inhibition of the membrane translocation of AKT. (B) Bar graph showing the analysis of fluorescence values in Fig. 3A ($n = 6$). (C) The effect of CA and CA4G on AKT enzymatic activity. (D) The effect of FA and FA4G on AKT enzymatic activity. The absorbance at 340 nm was detected continuously for 180 s to calculate AKT enzymatic activities. The values are expressed as the means ± SD ($n = 3$) ($^{**}P < 0.01$, $^{***}P < 0.001$ *vs* control group; $^{▲}P < 0.05$, $^{▲▲}P < 0.01$, $^{▲▲▲}P < 0.001$ *vs* parent compound group).

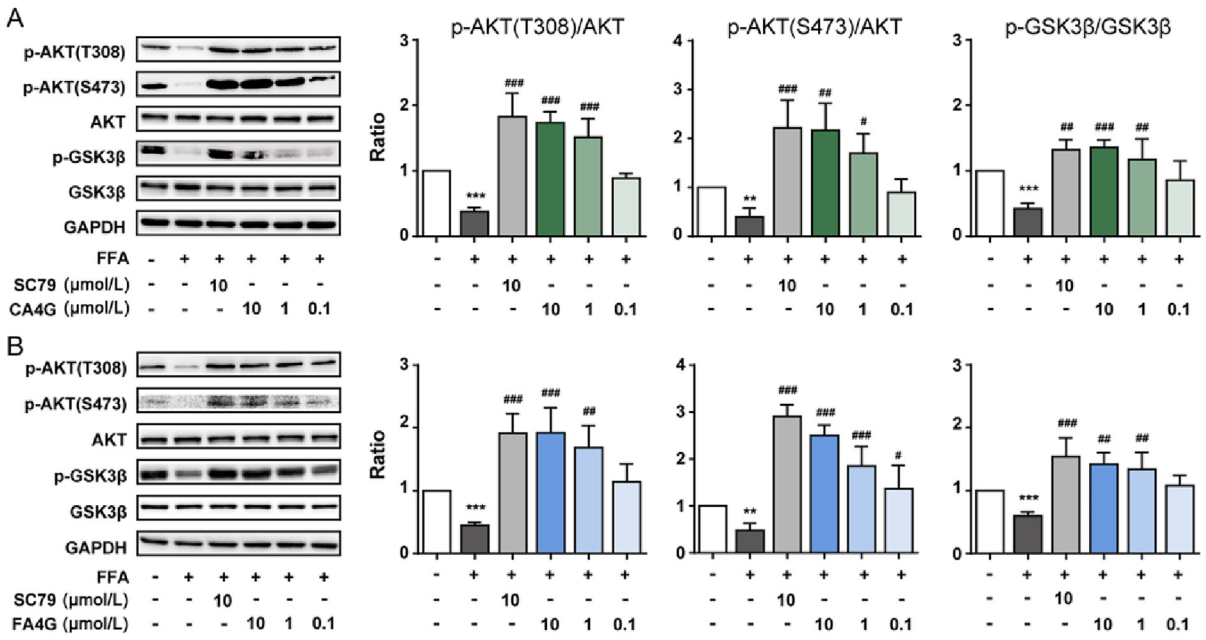

Fig. 4. Effect of CA4G and FA4G on p-AKT (T308), p-AKT (S473) and p-GSK3β. (A) The dose-dependent effect of CA4G (0.1–10 μmol/L) on the phosphorylation of AKT and GSK3β at 2 h after treatment. (B) The dose-dependent effect of FA4G (0.1–10 μmol/L) on the phosphorylation of AKT and GSK3β at 2 h after treatment. The values are expressed as the means ± SD (n = 3) ($^{**}P < 0.01$, $^{***}P < 0.001$ *vs* control group; $^{\#}P < 0.05$, $^{\#\#}P < 0.01$, $^{\#\#\#}P < 0.001$ *vs* insulin resistance model group).

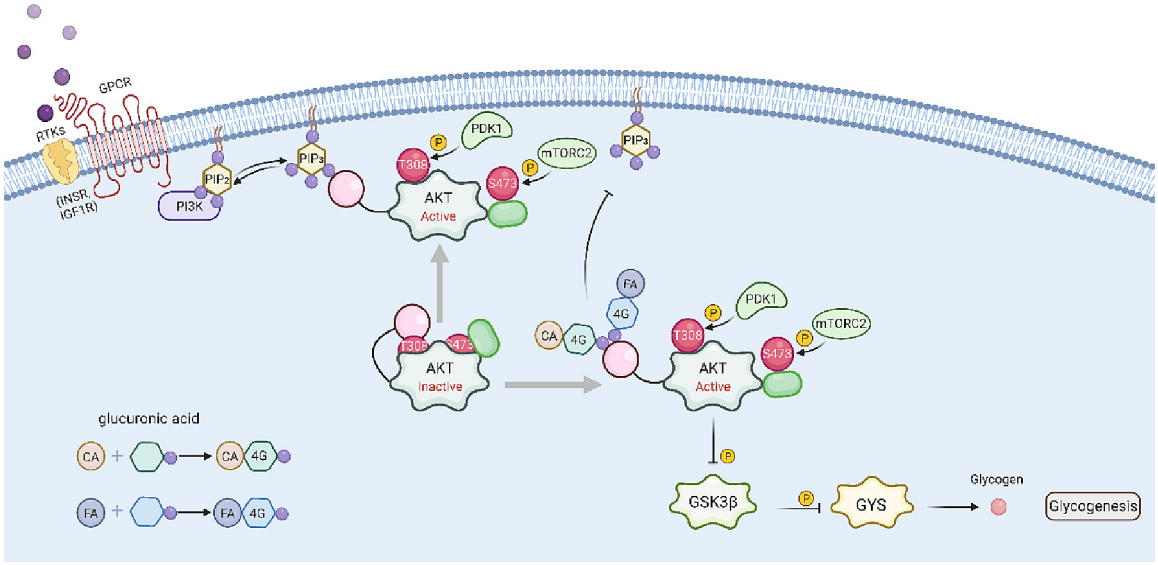

Fig. 5. CA4G and FA4G target the AKT PH domain to activate AKT, promote AKT phosphorylation, and improve glucose metabolism. Activated AKT regulates glucose metabolism through phosphorylation of GSK3β (Created with BioRender.com).

pate in the anticancer effect of polyphenols. Lee et al. reported that resveratrol activated natural killer (NK) cells by activating AKT via mTORC2 to defend against cancer (Lee & Kim, 2020). On the other hand, the mechanisms underlying the anticancer effect of polyphenols are commonly found to be related to their antioxidant and pro-oxidant capacities (Espindola et al., 2019).

5. Conclusion

In summary, this study found that glucuronic acid metabolites of phenolic acids showed better activity that their parent compounds in regulating glucose metabolism by binding to the PH domain to activate AKT and triggering the activation of downstream signaling pathways. Furthermore, the glucuronic structure might be the crucial group that interacts with the PH domain. The mechanism was predicted to be the glucuronic acid structure of the compounds binding to Arg-25 in AKT PH domain. This could be the common mechanism underlying the improved glucose metabolism exerted by glucuronic acid metabolites compared to their respective parent compounds. Our results provided evidence for further investigation to broaden the application of other glucuronic acid metabolites.

Declaration of Competing Interest

The authors declare that they have no known competing financial interests or personal relationships that could have appeared to influence the work reported in this paper.

Acknowledgments

This research was funded by Guangxi Innovation-driven Development 20 Special Foundation Project (No. AA18118049), Guangxi Key Laboratory of Efficacy Study on Chinese Materia Medica (19-245-1), and "the Fundamental Research Funds for the Central Universities" of Nankai University (No. 63191723).

References

Azuma, K., Ippoushi, K., Nakayama, M., Ito, H., Higashio, H., & Terao, J. (2000). Absorption of chlorogenic acid and caffeic acid in rats after oral administration. *Journal of Agricultural and Food Chemistry, 48*(11), 5496–5500.

Badolia, R., Manne, B. K., Dangelmaier, C., Chernoff, J., & Kunapuli, S. P. (2015). Gq-mediated Akt translocation to the membrane: A novel PIP3-independent mechanism in platelets. *Blood, 125*(1), 175–184.

Belwal, T., Nabavi, S. F., Nabavi, S. M., & Habtemariam, S. (2017). Dietary anthocyanins and insulin resistance: When food becomes a medicine. *Nutrients, 9*(10), 1111.

Boucher, J., Kleinridders, A., & Kahn, C. R. (2014). Insulin receptor signaling in normal and insulin-resistant states. *Cold Spring Harbor Perspectives in Biology, 6*(1), a009191.

Chang, W. C., Kuo, P. L., Chen, C. W., Wu, J. S. B., & Shen, S. C. (2015). Caffeic acid improves memory impairment and brain glucose metabolism via ameliorating cerebral insulin and leptin signaling pathways in high-fat diet-induced hyperinsulinemic rats. *Food Research International, 77*, 24–33.

Chen, L., Teng, H., & Cao, H. (2019). Chlorogenic acid and caffeic acid from *Sonchus oleraceus* Linn synergistically attenuate insulin resistance and modulate glucose uptake in HepG2 cells. *Food Chemical Toxicology, 127*, 182–187.

Chen, P., Song, M., Wang, Y., Deng, S., Hong, W., Zhang, X., & Yu, B. (2020). Identification of key genes of human bone marrow stromal cells adipogenesis at an early stage. *PeerJ, 8*, e9484.

Docampo-Palacios, M. L., Alvarez-Hernandez, A., de Fatima, A., Liao, L. M., Pasinetti, G. M., & Dixon, R. A. (2020). Efficient chemical synthesis of (Epi)catechin glucuronides: Brain-targeted metabolites for treatment of Alzheimer's disease and other neurological disorders. *Advanced Materials, 5*(46), 30095–30110.

Espindola, K. M. M., Ferreira, R. G., Narvaez, L. E. M., Silva Rosario, A. C. R., da Silva, A. H. M., Silva, A. G. B., ... Monteiro, M. C. (2019). Chemical and pharmacological aspects of caffeic acid and its activity in hepatocarcinoma. *Frontiers in Oncology, 9*, 541.

Fang, G., Cheng, C., Zhang, M., Ma, X., Yang, S., Hou, X., ... Bai, G. (2021). The glucuronide metabolites of kaempferol and quercetin, targeting to the AKT PH domain, activate AKT/GSK3β signaling pathway and improve glucose metabolism. *Journal of Functional Foods, 82*, 104501.

Ferguson, K. M., Kavran, J. M., Sankaran, V. G., Fournier, E., Isakoff, S. J., Skolnik, E. Y., & Lemmon, M. A. (2000). Structural basis for discrimination of 3-phosphoinositides by pleckstrin homology domains. *Molecular Cell, 6*(2), 373–384.

Gao, J., He, X., Ma, Y., Zhao, X., Hou, X., Hao, E., ... Bai, G. (2018). Chlorogenic acid targeting of the AKT PH domain activates AKT/GSK3beta/FOXO1 signaling and improves glucose metabolism. *Nutrients, 10*(10), 1366.

Huang, Y., Jin, M., Pi, R., Zhang, J., Chen, M., Ouyang, Y., ... Qin, J. (2013). Protective effects of caffeic acid and caffeic acid phenethyl ester against acrolein-induced neurotoxicity in HT22 mouse hippocampal cells. *Neuroscience Letters, 535*, 146–151.

Jiang, Z. Y., Zhou, Q. L., Coleman, K. A., Chouinard, M., Boese, Q., & Czech, M. P. (2003). Insulin signaling through Akt/protein kinase B analyzed by small interfering RNA-mediated gene silencing. *Proceedings of the National Academy of Sciences of the United States of America, 100*(13), 7569–7574.

Jo, H., Mondal, S., Tan, D., Nagata, E., Takizawa, S., Sharma, A. K., ... Luo, H. R. (2012). Small molecule-induced cytosolic activation of protein kinase Akt rescues ischemia-elicited neuronal death. *Proceedings of the National Academy of Sciences of the United States of America, 109*(26), 10581–10586.

Kumar, N., & Goel, N. (2019). Phenolic acids: Natural versatile molecules with promising therapeutic applications. *Biotechnology Reports, 24*, e00370.

Lafay, S., Morand, C., Manach, C., Besson, C., & Scalbert, A. (2006). Absorption and metabolism of caffeic acid and chlorogenic acid in the small intestine of rats. *British Journal of Nutrition, 96*(1), 39–46.

Lakowicz, J. R., & Weber, G. (1973). Quenching of fluorescence by oxygen. A probe for structural fluctuations in macromolecules. *Biochemistry, 12*(21), 4161–4170.

Lee, H. J., Lee, D. Y., Chun, Y. S., Kim, J. K., Lee, J. O., Ku, S. K., & Shim, S. M. (2022). Effects of blue honeysuckle containing anthocyanin on anti-diabetic hypoglycemia and hyperlipidemia in ob/ob mice. *Journal of Functional Foods, 89*, 104959.

Lee, Y.-J., & Kim, J. (2020). Resveratrol activates natural killer cells through Akt- and mTORC2-mediated c-Myb upregulation. *International Journal of Molecular Sciences, 21*(24), 9575.

Li, X., Wu, X., & Huang, L. (2009). Correlation between antioxidant activities and phenolic contents of *Radix Angelicae Sinensis* (Danggui). *Molecules, 14*(12), 5349–5361.

Manning, B. D., & Cantley, L. C. (2007). AKT/PKB signaling: Navigating downstream. *Cell, 129*(7), 1261–1274.

Manning, B. D., & Toker, A. (2017). AKT/PKB signaling: Navigating the network. *Cell, 169*(3), 381–405.

Narasimhan, A., Chinnaiyan, M., & Karundevi, B. (2015). Ferulic acid exerts its antidiabetic effect by modulating insulin-signalling molecules in the liver of high-fat diet and fructose-induced type-2 diabetic adult male rat. *Applied Physiology Nutrition Metabolism, 40*(8), 769–781.

Omar, M. H., Mullen, W., Stalmach, A., Auger, C., Rouanet, J. M., Teissedre, P. L., ... Crozier, A. (2012). Absorption, disposition, metabolism, and excretion of [3-(14) C]caffeic acid in rats. *Journal of Agricultural and Food Chemistry, 60*(20), 5205–5214.

Ovaskainen, M. L., Torronen, R., Koponen, J. M., Sinkko, H., Hellstrom, J., Reinivuo, H., & Mattila, P. (2008). Dietary intake and major food sources of polyphenols in Finnish adults. *Journal of Nutrition, 138*(3), 562–566.

Peillex, C., Kerever, A., Lachhab, A., & Pelletier, M. (2021). Bisphenol A, bisphenol S and their glucuronidated metabolites modulate glycolysis and functional responses of human neutrophils. *Environmental Research, 196*, 110336.

Pereira-Caro, G., Ludwig, I. A., Polyviou, T., Malkova, D., Garcia, A., Moreno-Rojas, J. M., & Crozier, A. (2016). Identification of plasma and urinary metabolites and catabolites derived from orange juice (poly)phenols: Analysis by high-performance liquid chromatography-high-resolution mass spectrometry. *Journal of Agricultural and Food Chemistry, 64*(28), 5724–5735.

Radisavljevic, Z. (2020). Lysosome AKT targeting in metastatic cancer. *Critical Reviews in Eukaryotic Gene Expression, 30*(2), 121–123.

Takeuchi, H., Kanematsu, T., Misumi, Y., Sakane, F., Konishi, H., Kikkawa, U., ... Hirata, M. (1997). Distinct specificity in the binding of inositol phosphates by pleckstrin homology domains of pleckstrin, RAC-protein kinase, diacylglycerol kinase and a new 130 kDa protein. *Biochimica et Biophysica Acta (BBA) - Molecular Cell Research, 1359*(3), 275–285.

Thomas, C. C., Deak, M., Alessi, D. R., & van Aalten, D. M. F. (2002). High-resolution structure of the pleckstrin homology domain of protein kinase B/Akt bound to phosphatidylinositol (3,4,5)-trisphosphate. *Current Biology, 12*(14), 1256–1262.

Tian, M., Xie, Y., Meng, Y., Ma, W., Tong, Z., Yang, X., ... Liao, Z. (2019). Resveratrol protects cardiomyocytes against anoxia/reoxygenation via dephosphorylation of VDAC1 by Akt-GSK3 beta pathway. *European Journal Pharmacology, 843*, 80–87.

Titchenell, P. M., Quinn, W. J., Lu, M., Chu, Q., Lu, W., Li, C., ... Birnbaum, M. J. (2016). Direct hepatocyte insulin signaling is required for lipogenesis but is dispensable for the suppression of glucose production. *Cell Metabolism, 23*(6), 1154–1166.

Tsai, Y. F., Chen, C. Y., Chang, W. Y., Syu, Y. T., & Hwang, T. L. (2019). Resveratrol suppresses neutrophil activation via inhibition of Src family kinases to attenuate lung injury. *Free Radical Biology and Medicine, 145*, 67–77.

Tumova, S., Shi, Y., Carr, I. M., & Williamson, G. (2021). Effects of quercetin and metabolites on uric acid biosynthesis and consequences for gene expression in the endothelium. *Free Radical Biology and Medicine, 162*, 191–201.

Wang, L., Fan, Y., Mei, H., Liu, Y., Zhang, L., Xu, J., & Huang, X. (2019). Novel Hsp90 inhibitor C086 potently inhibits non-small cell lung cancer cells as a single agent or in combination with gefitinib. *Cancer Management and Research, 11*, 8937–8945.

Xie, K., Jin, B., Zhu, H., Zhou, P., Du, L., & Jin, X. (2020). Ferulic acid (FA) protects human retinal pigment epithelial cells from H2O2 -induced oxidative injuries. *Journal of Cellular and Molecular Medicine, 24*(22), 13454–13462.

Yang, S., Zhang, Y., Shen, F., Ma, X., Zhang, M., Hou, Y., & Bai, G. (2019). The flavonoid baicalin improves glucose metabolism by targeting the PH domain of AKT and activating AKT/GSK3beta phosphorylation. *FEBS Letters, 593*(2), 175–186.

Yin, C. L., Lu, R. G., Zhu, J. F., Huang, H. M., Liu, X., Li, Q. F., ... Zheng, H. (2019). The study of neuroprotective effect of ferulic acid based on cell metabolomics. *European Journal of Pharmacology, 864*, 172694.

Zhan, Y. F., Hou, X. T., Fan, L. L., Du, Z. C., Ch'ng, S. E., Ng, S. M., ... Deng, J. G. (2021). Chemical constituents and pharmacological effects of durian shells in ASEAN countries: A review. *Chinese Herbal Medicines, 13*(4), 461–471.

Zhang, M., Ma, X., Xu, H., Wu, W., He, X., Wang, X., ... Bai, G. (2020). A natural AKT inhibitor swertiamarin targets AKT-PH domain, inhibits downstream signaling, and alleviates inflammation. *FEBS Journal, 287*(9), 1816–1829.

Zhang, Y., Yan, L. S., Ding, Y., Cheng, B. C. Y., Luo, G., Kong, J., ... Zhang, S. F. (2019). *Edgeworthia gardneri* (Wall.) Meisn. water extract ameliorates palmitate induced insulin resistance by regulating IRS1/GSK3beta/FoxO1 signaling pathway in human HepG2 hepatocytes. *Frontiers in Pharmacology, 10*, 1666.

Zhang, Y., Yang, S., Zhang, M., Wang, Z., He, X., Hou, Y., & Bai, G. (2019). Glycyrrhetinic acid improves insulin-response pathway by regulating the balance between the Ras/MAPK and PI3K/Akt pathways. *Nutrients, 11*(3), 604.

Zhao, Z., Egashira, Y., & Sanada, H. (2004). Ferulic acid is quickly absorbed from rat stomach as the free form and then conjugated mainly in liver. *Journal of Nutrition, 134*(11), 3083–3088.

Zhao, Z., & Moghadasian, M. H. (2008). Chemistry, natural sources, dietary intake and pharmacokinetic properties of ferulic acid: A review. *Food Chemistry, 109*(4), 691–702.